

## Bimetallic Derivatives of $[M(en)_3]^{3+}$ Ions ( $M = Cr, Co$ ): An Approach to Intermolecular Magnetic Interactions in Molecular Magnets

M. Carmen Morón,<sup>1a</sup> Fernando Palacio,<sup>\*1a</sup> J. Pons,<sup>1b</sup> J. Casabó,<sup>1b</sup> X. Solans,<sup>1c</sup> K. E. Merabet,<sup>1d</sup> D. Huang,<sup>1d</sup> X. Shi,<sup>1d</sup> Boon K. Teo,<sup>1d</sup> and Richard L. Carlin<sup>\*1d</sup>

Instituto de Ciencia de Materiales de Aragón, CSIC-Universidad de Zaragoza, 50009 Zaragoza, Spain, Instituto de Ciencia de Materiales de Barcelona, CSIC and Departament de Química Inorgànica, Universidad Autònoma de Barcelona, Bellaterra, Spain, Department of Crystallography, Universidad de Barcelona, 08028 Barcelona, Spain, and Department of Chemistry, University of Illinois at Chicago, Chicago, Illinois 60680

Received July 8, 1993\*

The crystal and molecular structures together with the magnetic susceptibilities of a series of  $[M(en)_3]^{3+}$  ( $M = Cr, Co$ ) derivatives are reported. The space group and unit cell dimensions of  $[Cr(en)_3]_3[FeCl_6]Cl_6 \cdot H_2O$  (1),  $[Co(en)_3]_3[FeCl_6]Cl_6 \cdot H_2O$  (2), and  $[Cr(en)_3][FeCl_4]Cl_2 \cdot 9H_2O$  (3) are as follows: (1)  $R3$ ,  $a = 15.445(4)$  Å,  $c = 21.060(6)$  Å,  $Z = 3$ ; (2)  $R3$ ,  $a = 15.346(3)$  Å,  $c = 20.880(5)$  Å,  $Z = 3$ ; (3)  $P3c1$ ,  $a = 11.654(3)$  Å,  $c = 15.508(4)$  Å,  $Z = 2$ . The trigonal crystal structures contain discrete  $[M(en)_3]^{3+}$  ( $M = Cr, Co$ ),  $[FeCl_6]^{3-}$ , and  $Cl^-$  ions and water molecules. With no covalent bonds connecting the iron and chromium (or cobalt) sublattices, the complex cations, anions, and water molecules are held together by ionic forces and by a three-dimensional network of hydrogen bonds. The magnetic susceptibilities of 1, 2,  $[M(en)_3][FeCl_6]$  ( $M = Cr, Co$ ), and  $[Cr(en)_3][InCl_6]$  are also reported. While 1 orders as a ferrimagnet at 0.91 K, with  $J_{Fe-Cr}/k_B = -0.153$  K,  $J_{Fe-Fe}/k_B = -0.044$  K, and  $J_{Cr-Cr}/k_B = -0.045$  K,  $[Co(en)_3][FeCl_6]$  exhibits antiferromagnetic properties below  $T_c = 1.43$  K and  $[Cr(en)_3][FeCl_6]$  evidences antiferromagnetic-like (compensated ferrimagnetic) ordering with  $(d\chi/dT)_{max} = 2.26$  K. The data were interpreted in terms of the interaction Hamiltonian  $H = -2\sum_{i<j} J_{ij} S_i S_j$ . Structural and magnetic properties are correlated by investigating the superexchange pathways through which the magnetic moments interact and magnetic ordering is established. As a result, hydrogen bonds are shown to be an effective mechanism to propagate magnetic interactions in these molecular magnets.

### Introduction

One of the major problems in contemporary magnetochemistry is the design and successful synthesis of molecular ferromagnets and ferrimagnets.<sup>2</sup> The synthesis of molecular ferromagnets constitutes a difficult task, since magnetic interactions in these solids are commonly transmitted by means of the superexchange mechanism which strongly favors antiparallel alignment of the magnetic moments in this type of compound. On the other hand, a ferrimagnet can be considered, in a simplified picture, as an antiferromagnet in which the magnetic sublattices do not compensate each other. Then, the synthesis of molecular ferrimagnets provides a convenient strategy to overcome the difficulties related with parallel alignment of the moments found preparing ferromagnets.<sup>3</sup> Efforts to prepare new bimetallic ferrimagnets must rely either upon heterometallic substances or else upon homometallic compounds possessing a distinct magnetic moment for each counterion.<sup>4-8</sup>

Complex bimetallic salts are of interest because the large number of complex ions available provides a variety of materials exhibiting different magnetic properties. In particular, when both complex ions are magnetic and differ in the magnitude of their moments, ferrimagnetism may arise below the ordering temperature, which in general is expected to be low in this type of substance. Ferrimagnetic systems undergoing magnetic ordering at low temperatures are of interest because they can permit accurate thermodynamic studies. That is because most ferrimagnetic materials already known order at relatively high temperatures and, consequently, possess a large phonon contribution to the specific heat as compared to the magnetic one. As a result, there are very few experimental studies of the specific heat of ferrimagnets.<sup>9,10</sup>

The study of a ferrimagnetic system implies the determination of quite a few parameters. In addition to the exchange interaction between magnetic sublattices, magnetic interactions, either ferro or antiferromagnetic, may be present within each sublattice. Moreover, each sublattice possesses its own magnetic moment which accounts for two values of the spin and two  $g$ -factors. In order to overcome such a number of parameters it is useful to study equivalent magnetic systems in which one paramagnetic counterion is substituted by a diamagnetic analogue. Then, one can determine the magnetic behavior which separately corresponds

\* Abstract published in *Advance ACS Abstracts*, January 15, 1994.

- (1) (a) Consejo Superior de Investigaciones Científicas (CSIC) and University of Zaragoza. (b) CSIC and University Autònoma de Barcelona. (c) University of Barcelona. (d) University of Illinois at Chicago.
- (2) Gatteschi, D.; Kahn, O.; Miller, J. S.; Palacio, F. *Magnetic Molecular Materials*; Kluwer Acad. Publ.: Dordrecht, The Netherlands, 1990; Vol. E198.
- (3) Kahn, O. In *Magnetic molecular materials*; Gatteschi, D., Kahn, O. J. Miller, Jr., Palacio, F., Eds.; Kluwer Acad. Publ.: Dordrecht, The Netherlands, 1991; Vol. E198, p 35.
- (4) Landee, C. P. In *Organic and Inorganic Low-Dimensional Crystalline Materials*; Delhaes, P., Drillon, M., Eds.; Plenum Publ. Corp.: New York, 1987; Vol. B168, p 75.
- (5) Kahn, O. In *Organic and Inorganic Low-Dimensional Crystalline Materials*; Delhaes, P., Drillon, M., Eds.; Plenum Publ. Corp.: New York, 1987; Vol. B168, p 93.
- (6) Caneschi, A.; Gatteschi, D.; Renard, J. P.; Rey, P.; Sessoli, R. *J. Am. Chem. Soc.* **1989**, *111*, 785.

- (7) Caneschi, A.; Gatteschi, D.; Sessoli, R.; Rey, P. *Acc. Chem. Res.* **1989**, *22*, 392.
- (8) Coronado, E. In *Magnetic Molecular Materials*; Gatteschi, D., Kahn, O., Miller, J. S., Palacio, F., Eds.; Kluwer Acad. Publ.: Dordrecht, The Netherlands, 1990; Vol. E198, p 267.
- (9) Drillon, M.; Coronado, E.; Beltrán, D.; Curely, J.; Georges, R.; Nugteren, P. R.; de Jongh, L. J.; Genicon, J. L. *J. Magn. Magn. Mater.* **1986**, *54-57*, 1507.
- (10) Coronado, E.; Nugteren, P. R.; Drillon, M.; Beltrán, D.; de Jongh, L. J.; Georges, R. In *Organic and Inorganic Low-Dimensional Crystalline Materials*; Delhaes, P., Drillon, M., Eds.; Plenum Press: New York, 1987; Vol. B168, p 405.

to each sublattice. One of the great advantages of dealing with bimetallic salts is the fairly large number of counterions that can be used as building blocks of magnetic materials. The building blocks in the construction of the magnetic materials here described have been  $[M(en)_3]$  and  $[M'Cl_6]$ , where  $M = Cr$  or  $Co$  and  $M' = Fe$  or  $In$ .

Complex bimetallic salts have some more appealing features. In these salts complex ions are used as building blocks yielding materials generally possessing rather symmetric structures, since ionic radii are in most cases of comparable size. Magnetic interactions in these substances are always intermolecular, and it is possible to establish the superexchange pathways since the crystal structures can often be determined. Such a possibility is not a common feature in most nonpolymeric molecular materials where the absence of covalent bonds complicates the superexchange pathways through which magnetic interactions are transmitted. However, to correlate magnetic ordering with structural properties is of interest because it contributes to a better understanding of the way intermolecular interactions propagate in these materials.

The magnetic properties of few three-dimensional complex bimetallic compounds have been studied.<sup>11-13</sup> As part of our search concerning complex bimetallic salts<sup>14-17</sup> and in particular new low-temperature ferrimagnets,<sup>18,19</sup> we attempted to prepare single crystals of  $[Cr(en)_3][FeCl_6]$ , where  $en$  is 1,2-ethanediamine. The system seemed very promising after (antiferromagnetic) ordering was reported in  $[Co(pn)_3][FeCl_6]$ , where  $pn$  is 1,2-propanediamine and  $Co^{3+}$  is a diamagnetic ion.<sup>11</sup> In almost every attempt, deep-red crystals of a substance of formula  $[Cr(en)_3]_3[FeCl_6]Cl_6 \cdot H_2O$  were in fact grown. Only in one exceptional case, some small crystals of what turned out to be  $[Cr(en)_3][FeCl_4]Cl_2 \cdot 9H_2O$  appeared.  $[Cr(en)_3][FeCl_6]$  could be prepared only as a powdered precipitate.

We report here the synthesis, crystal structure, and magnetic properties of the complex bimetallic salts  $[M(en)_3]_3[FeCl_6]Cl_6 \cdot H_2O$ , ( $M = Cr$  (1),  $Co$  (2)). Moreover, the crystal structure of  $[Cr(en)_3][FeCl_4]Cl_2 \cdot 9H_2O$  (3) and the magnetic properties of  $[M(en)_3][M'Cl_6]$ , ( $M = Cr, Co$ ;  $M' = Fe, In$ ) are also reported. The magnetic behavior of 3 is not given since the crystals were too small for magnetic susceptibility measurements and the powder could not be isolated. Finally, we devote some effort to study the magneto-structural correlations in these materials to acquire a better understanding of intermolecular exchange interactions in these molecular-like systems.

## Results

**Crystal Structures.** The crystal structures of 1-3 have been solved by X-ray single-crystal diffraction. No crystals of  $[M(en)_3][M'Cl_6]$  ( $M = Cr, Co$ ;  $M' = Fe, In$ ) were available. A summary of crystal data collection and structure refinement is given in Table 1 for 1-3. Significant atomic positions, bond lengths and angles are shown in Tables 2 and 3, 4 and 5, and 6 and 7 for compounds 1-3, respectively. Less important structural information of this type and anisotropic thermal parameters are available as supplementary material (Tables S1-S10).

- Scoville, A. N.; Lazar, K.; Reiff, W. M.; Landee, C. *Inorg. Chem.* **1983**, *22*, 3514.
- Helms, J. H.; Hatfield, W. E.; Kwiecien, M. J.; Reiff, W. M. *J. Chem. Phys.* **1986**, *84*, 3993.
- Carlin, R. L. *Comments Inorg. Chem.* **1991**, *11*, 215.
- Morón, M. C.; Palacio, F.; Pons, J.; Casabó, J.; Merabet, K. E.; Carlin, R. L. *J. Appl. Phys.* **1988**, *63*, 3566.
- Pons, J.; Casabó, J.; Palacio, F.; Morón, M. C.; Solans, X.; Carlin, R. L. *Inorg. Chim. Acta* **1988**, *146*, 161.
- Morón, M. C.; Palacio, F.; Navarro, R.; Pons, J.; Casabó, J.; Carlin, R. L. *Inorg. Chem.* **1990**, *29*, 842.
- Morón, M. C.; Palacio, F.; Pons, J.; Casabó, J.; Carlin, R. L. *Eur. J. Solid State Inorg. Chem.* **1991**, *28*, 431.
- Palacio, F.; Morón, M. C.; Pons, J.; Casabó, J.; Merabet, K. E.; Carlin, R. L. *Phys. Lett. A* **1989**, *135*, 231.
- Morón, M. C.; Palacio, F.; Pons, J.; Casabó, J. *J. Magn. Magn. Mater.* **1992**, *114*, 243.

**Table 1.** Summary of Crystal Data Collection and Structure Refinement for 1-3<sup>a</sup>

	compd		
	1	2	3
space group	R3 (No. 146)	R3 (No. 146)	P3c1 (No. 158)
<i>a</i> (Å)	15.445(4)	15.346(3)	11.654(3)
<i>c</i> (Å)	21.060(6)	20.880(5)	15.508(4)
<i>V</i> (Å <sup>3</sup> )	4353(4)	4258(3)	1824(1)
<i>Z</i>	3	3	2
<i>fw</i>	1196.2	1217.0	663.0
$\rho$ (g cm <sup>-3</sup> )	1.369	1.423	1.207
$\lambda$ (Å)	0.71069	0.71069	0.71069
<i>T</i> (°C)	23	15	25
$\mu$ (cm <sup>-1</sup> )	13.72	17.46	11.94
<i>R</i> <sup>b</sup>	0.048	0.044	0.040
<i>R</i> <sub>w</sub> <sup>c</sup>	0.052	0.051	0.040

<sup>a</sup> **1** =  $[Cr(en)_3]_3[FeCl_6]Cl_6 \cdot H_2O$ , **2** =  $[Co(en)_3]_3[FeCl_6]Cl_6 \cdot H_2O$ , and **3** =  $[Cr(en)_3][FeCl_4]Cl_2 \cdot 9H_2O$ . <sup>b</sup>  $R = \sum(|F_o| - |F_c|) / \sum |F_o|$ . <sup>c</sup>  $R_w = \{ \sum [w(|F_o| - |F_c|)^2] / \sum w |F_o|^2 \}^{1/2}$ .

**Table 2.** Significant Atomic Coordinates ( $\times 10^4$ ) for  $[Cr(en)_3]_3[FeCl_6]Cl_6 \cdot H_2O$

atom	site	x	y	z
Fe	3a	0	0	0
Cl(1)	9b	776(2)	1478(2)	643(1)
Cl(2)	9b	-779(2)	699(2)	-648(1)
Cr	9b	3332(1)	1446(1)	1666(1)
N(1)	9b	3700(6)	1704(7)	2607(4)
N(2)	9b	2308(7)	1870(8)	1937(5)
N(3)	9b	2338(7)	-47(7)	1830(5)
N(4)	9b	4310(7)	951(8)	1479(5)
N(5)	9b	4377(7)	2917(9)	1398(5)
N(6)	9b	2968(7)	1304(8)	694(5)

**Table 3.** Significant Interatomic Distances (Å) and Angles (deg) for  $[Cr(en)_3]_3[FeCl_6]Cl_6 \cdot H_2O$

Iron Coordination Sphere			
Distances			
Fe-Cl(1)	2.396(2)	Fe-Cl(2)	2.402(3)
Angles			
Cl(1)-Fe-Cl(1)	91.20(8)	Cl(2)-Fe-Cl(2)	90.94(8)
Cl(1)-Fe-Cl(2)	91.0(1)	Cl(2)-Fe-Cl(1)	86.94(8)
Chromium Coordination Sphere			
Distances			
Cr-N(1)	2.05(1)	Cr-N(2)	2.07(1)
Cr-N(3)	2.06(1)	Cr-N(4)	2.04(1)
Cr-N(5)	2.10(1)	Cr-N(6)	2.10(1)
Angles			
N(1)-Cr-N(2)	81.5(4)	N(1)-Cr-N(3)	92.0(4)
N(1)-Cr-N(4)	94.3(5)	N(1)-Cr-N(5)	93.5(4)
N(1)-Cr-N(6)	175.1(5)	N(2)-Cr-N(3)	92.8(5)
N(2)-Cr-N(4)	174.4(4)	N(2)-Cr-N(5)	91.5(5)
N(2)-Cr-N(6)	95.4(5)	N(3)-Cr-N(4)	83.7(4)
N(3)-Cr-N(5)	173.4(5)	N(3)-Cr-N(6)	92.0(4)
N(4)-Cr-N(5)	92.3(5)	N(4)-Cr-N(6)	89.0(5)
N(5)-Cr-N(6)	82.6(4)		
Hydrogen Bonding			
N(3)-Cl(1)	3.32(1)	N(6)-Cl(1)	3.366(9)
N(4)-Cl(2)	3.37(1)	N(1)-Cl(2)	3.39(1)
N(5)-Cl(2)	3.43(1)	N(2)-Cl(1)	3.46(1)
N(6)-Cl(2)	3.47(1)	N(1)-Cl(2)	3.495(8)
N(1)-Cl(1)	3.515(8)	N(6)-Cl(1)	3.53(1)

**$[Cr(en)_3]_3[FeCl_6]Cl_6 \cdot H_2O$  and  $[Co(en)_3]_3[FeCl_6]Cl_6 \cdot H_2O$ .** The crystal structure of compound 1 contains discrete  $[Cr(en)_3]^{3+}$ ,  $[FeCl_6]^{3-}$ , and  $Cl^-$  ions as well as isolated water molecules. The packing of the atoms is shown in Figures 1 and 2.

The nearly octahedral coordination polyhedron about the chromium atom is built up of six nitrogen atoms from three 1,2-ethanediamine ligands. The six independent Cr-N bond distances range from 2.04(1) to 2.10(1) Å. This gives an average Cr-N distance of  $d_{Cr-N} = 2.07$  Å in excellent agreement with those

**Table 4.** Significant Atomic Coordinates ( $\times 10^4$ ) for  $[\text{Co}(\text{en})_3][\text{FeCl}_6]\text{Cl}_6\cdot\text{H}_2\text{O}$ 

atom	site	x	y	z
Fe	3a	0	0	0
Cl(1)	9b	692(1)	1477(1)	653(1)
Cl(2)	9b	-690(1)	788(1)	-646(1)
Co	9b	8097(1)	1430(1)	1673(1)
N(1)	9b	7936(4)	1683(4)	2552(2)
N(2)	9b	9483(4)	1813(5)	1897(3)
N(3)	9b	8319(4)	1277(4)	749(2)
N(4)	9b	8522(4)	2852(4)	1438(3)
N(5)	9b	6666(3)	971(4)	1490(2)
N(6)	9b	7668(4)	31(4)	1842(3)

**Table 5.** Significant Interatomic Distances ( $\text{\AA}$ ) and Angles (deg) for  $[\text{Co}(\text{en})_3][\text{FeCl}_6]\text{Cl}_6\cdot\text{H}_2\text{O}$ 

Iron Coordination Sphere			
Distances			
Fe-Cl(1)	2.391(1)	Fe-Cl(2)	2.384(1)
Angles			
Cl(1)-Fe-Cl(1)	90.7(1)	Cl(2)-Fe-Cl(2)	91.1(1)
Cl(1)-Fe-Cl(2)	91.7(1)	Cl(2)-Fe-Cl(1)	86.6(1)
Cobalt Coordination Sphere			
Distances			
Co-N(1)	1.919(5)	Co-N(2)	1.959(5)
Co-N(3)	1.992(5)	Co-N(4)	2.002(5)
Co-N(5)	1.979(5)	Co-N(6)	1.937(5)
Angles			
N(1)-Co-N(2)	86.6(3)	N(1)-Co-N(3)	175.7(3)
N(1)-Co-N(4)	91.0(3)	N(1)-Co-N(5)	91.4(3)
N(1)-Co-N(6)	92.5(3)	N(2)-Co-N(3)	92.4(3)
N(2)-Co-N(4)	91.0(3)	N(2)-Co-N(5)	176.2(3)
N(2)-Co-N(6)	90.3(3)	N(3)-Co-N(4)	84.8(3)
N(3)-Co-N(5)	89.8(3)	N(3)-Co-N(6)	91.7(3)
N(4)-Co-N(5)	92.2(3)	N(4)-Co-N(6)	176.3(3)
N(5)-Co-N(6)	86.5(3)		
Hydrogen Bonding			
N(1)-Cl(2)	3.309(7)	N(6)-Cl(1)	3.331(7)
N(3)-Cl(1)	3.338(7)	N(5)-Cl(2)	3.345(6)
N(2)-Cl(1)	3.378(7)	N(4)-Cl(2)	3.378(7)
N(1)-Cl(2)	3.454(7)	N(3)-Cl(1)	3.504(7)

**Table 6.** Significant Atomic Coordinates ( $\times 10^4$ ) for  $[\text{Cr}(\text{en})_3][\text{FeCl}_4]\text{Cl}_2\cdot 9\text{H}_2\text{O}$ 

atom	site	x	y	z
Fe	2b	$1/3$	$2/3$	6632(2)
Cl(1)	6d <sup>a</sup>	1795(4)	7213(6)	2315(2)
Cl(2)	6d <sup>a</sup>	1832(3)	4454(8)	1070(2)
Cr	2c	$2/3$	$1/3$	4122(0)
N(1)	6d	6789(9)	1889(9)	3351(4)
N(2)	6d	8002(8)	3077(9)	4914(4)
O(1)	6d	8979(10)	4029(12)	1623(5)
O(1')	6d	4941(15)	4023(16)	1657(6)
O(2)	6d	3875(4)	8995(4)	4141(3)
O(3)	6d	1252(4)	2550(4)	4142(3)

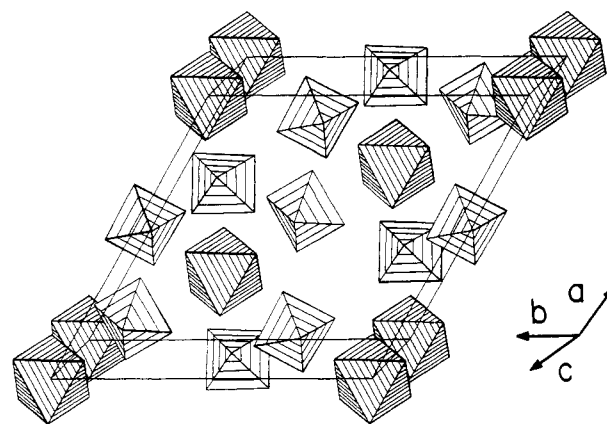
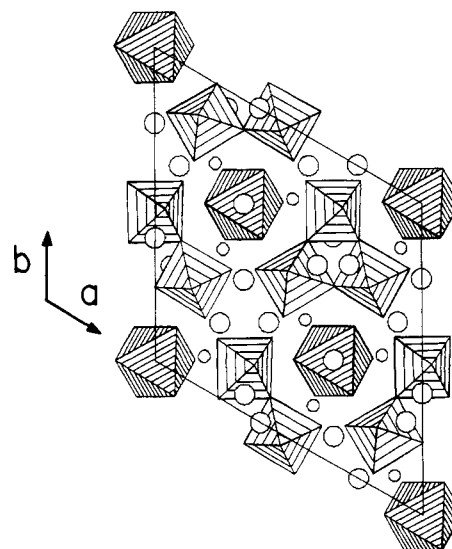
<sup>a</sup> Occupancy factor  $2/3$ .

found in related bimetallic salts as  $[\text{Cr}(\text{NH}_3)_6][\text{MnCl}_5\text{H}_2\text{O}]$ ,<sup>20</sup>  $[\text{Cr}(\text{NH}_3)_6][\text{ZnCl}_4]\text{Cl}$ ,<sup>21</sup>  $[\text{Cr}(\text{NH}_3)_6][\text{HgCl}_5]$ ,<sup>22</sup>  $[\text{Cr}(\text{NH}_3)_6][\text{FeF}_6]$ ,<sup>23</sup> and  $[\text{Cr}(\text{NH}_3)_6][\text{Ni}(\text{H}_2\text{O})_6]\text{Cl}_3\cdot 1/2\text{NH}_4\text{Cl}$ .<sup>24</sup>

The iron atom is located on the 3-fold axis and surrounded by six chlorine atoms in a fairly regular octahedral arrangement. There are only two independent  $d_{\text{Fe-Cl}}$  bond lengths, 2.396(2) and 2.402(3)  $\text{\AA}$ , which compare very well with those found in related compounds as  $[\text{Co}(\text{NH}_3)_6][\text{FeCl}_6]$ <sup>25</sup> and  $\text{Cs}_2\text{NaFeCl}_6$ .<sup>26</sup> It seems

(20) Clegg, W. *Acta Crystallogr. B* **1978**, *34*, 3328.(21) Clegg, W. *Acta Crystallogr. B* **1976**, *32*, 2907.(22) Clegg, W.; Greenhalgh, D. A.; Straughan, B. P. *J. Chem. Soc., Dalton Trans.* **1975**, 2591.(23) Wiegardt, V. K.; Weiss, J. *Acta Crystallogr. B* **1972**, *28*, 529.(24) Morón, M. C.; Le Bail, A.; Pons, J. J. *Solid State Chem.* **1990**, *88*, 498.**Table 7.** Significant Interatomic Distances ( $\text{\AA}$ ) and Angles (deg) for  $[\text{Cr}(\text{en})_3][\text{FeCl}_4]\text{Cl}_2\cdot 9\text{H}_2\text{O}$ 

Iron Coordination Sphere			
Distances			
Fe-Cl(1)	2.425(6)	Fe-Cl(2)	2.441(7)
Angles			
Cl(1)-Fe-Cl(1)	102.3(1)	Cl(2)-Fe-Cl(2)	108.0(1)
Cl(1)-Fe-Cl(2)	101.5(2)		
Chromium Coordination Sphere			
Distances			
Cr-N(1)	2.126(1)	Cr-N(2)	2.117(1)
Angles			
N(1)-Cr-N(1)	91.5(3)	N(2)-Cr-N(2)	88.5(3)
N(1)-Cr-N(2)	82.5(3)		
Hydrogen Bonding			
Cl(1)-O(1')	3.07(2)	Cl(2)-O(1)	3.22(1)
N(1)-O(1')	2.83(1)	N(2)-O(1')	2.95(1)
N(1)-O(1)	3.20(1)	N(2)-O(1)	3.25(1)

**Figure 1.** Arrangement of  $[\text{Cr}(\text{en})_3]^{3+}$  (light hatching) and  $[\text{FeCl}_6]^{3-}$  (heavy hatching) polyhedra in  $[\text{Cr}(\text{en})_3]_3[\text{FeCl}_6]\text{Cl}_6\cdot\text{H}_2\text{O}$ .**Figure 2.** Projection of the structure of  $[\text{Cr}(\text{en})_3]_3[\text{FeCl}_6]\text{Cl}_6\cdot\text{H}_2\text{O}$  on the (001) plane. The octahedra represent  $[\text{Cr}(\text{en})_3]^{3+}$  cations (light hatching) and  $[\text{FeCl}_6]^{3-}$  anions (heavy hatching). Isolated chlorine atoms and water molecules are represented by large and small circles, respectively.

worth remarking that the spatial distribution of the  $[\text{FeCl}_6]^{3-}$  octahedra is very similar to that found for the  $[\text{Cr}(\text{NH}_3)_6]^{3+}$  octahedra in  $[\text{Cr}(\text{NH}_3)_6][\text{ZnCl}_4]\text{Cl}$ .<sup>21</sup>

(25) Beattie, J. K.; Moore, C. J. *Inorg. Chem.* **1982**, *21*, 1292.(26) Verbist, J. J.; Hamilton, W. C.; Koetzle, T. F.; Lehmann, M. S. *J. Chem. Phys.* **1972**, *56*, 3257.

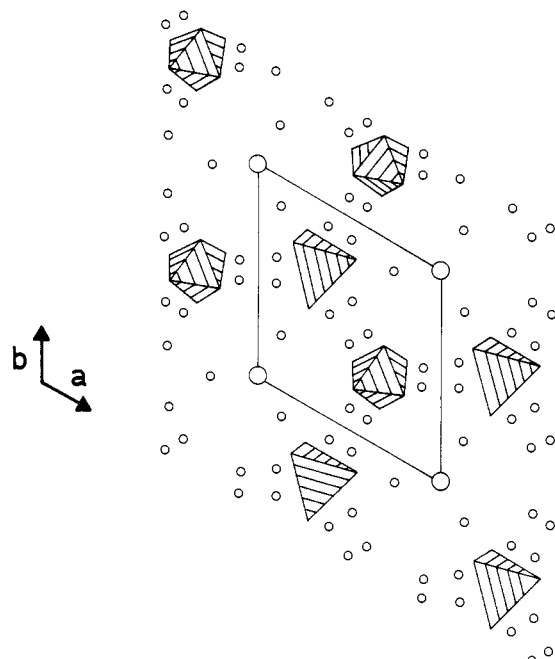


**Figure 3.** Projection of the structure of  $[\text{Cr}(\text{en})_3][\text{FeCl}_4]\text{Cl}_2 \cdot 9\text{H}_2\text{O}$  on the (001) plane. The octahedra represent  $[\text{Cr}(\text{en})_3]^{3+}$  cations, and the tetrahedra,  $[\text{FeCl}_4]^-$  anions. Isolated  $\text{Cl}^-$  anions and water molecules are represented by large and small circles, respectively.

The complex cations, anions, and water molecules are held together by ionic forces and by a three-dimensional network of hydrogen bonds. The  $[\text{Cr}(\text{en})_3]^{3+}$  cations are linked to the  $[\text{FeCl}_4]^-$  and  $\text{Cl}^-$  anions through  $\text{N}\cdots\text{Cl}$  hydrogen bonds, while the  $\text{H}_2\text{O}$  molecules are also related to the isolated  $\text{Cl}^-$  ions by means of  $\text{O}\cdots\text{Cl}$  contacts.

The similarity between the coordination chemistry of octahedral chromium(III) and cobalt(III) ions is well established. Therefore, it is not surprising that similar synthetic paths lead to the related compounds **1** and **2** and that both compounds present an isomorphous distribution of the complex ions. The isomorphism between crystal structures of compounds containing either octahedral chromium(III) or cobalt(III) ions is a common phenomena, as shown, for example, by the pairs  $[\text{Cr}(\text{NH}_3)_6][\text{CuCl}_5]^{27}$  and  $[\text{Co}(\text{NH}_3)_6][\text{CuCl}_5]^{28}$  or  $[\text{Co}(\text{NH}_3)_6][\text{Cr}(\text{CN})_6]^{29}$  and  $[\text{Co}(\text{NH}_3)_6][\text{Co}(\text{CN})_6]^{30}$ . The six independent  $d_{\text{Co-N}}$  bond distances range from 1.919(5) Å to 2.002(5) Å and average 1.965 Å, in excellent agreement with those found in related bimetallic salts as  $[\text{Co}(\text{NH}_3)_6][\text{FeCl}_6]^{25}$ ,  $[\text{Co}(\text{NH}_3)_6][\text{CuCl}_5]^{28}$  and  $[\text{Co}(\text{NH}_3)_6][\text{CdCl}_5]^{31}$ .

**$[\text{Cr}(\text{en})_3][\text{FeCl}_4]\text{Cl}_2 \cdot 9\text{H}_2\text{O}$ .** The crystal structure of **3** contains discrete  $[\text{Cr}(\text{en})_3]^{3+}$ ,  $[\text{FeCl}_4]^-$ , and  $\text{Cl}^-$  ions as well as isolated water molecules. The packing of the atoms is shown in Figure 3.

Chromium and iron ions are both located on the 3-fold axis in octahedral and tetrahedral sites, respectively. The spatial distribution of ions in **3** is consistent with an arrangement of parallel stacks of  $[\text{Cr}(\text{en})_3]^{3+}$  and  $[\text{FeCl}_4]^-$  aligned parallel to the (001) axis as shown in Figure 3. Analogous stacklike arrangements can be found in  $[\text{Co}(\text{NH}_3)_6][\text{FeCl}_6]^{25}$  and  $[\text{Cr}(\text{NH}_3)_6][\text{Ni}(\text{H}_2\text{O})_6]\text{Cl}_5 \cdot 1/2\text{NH}_4\text{Cl}^{24}$ . However, in these two compounds each stack is built up by alternating counterions.

The cations, anions, and water molecules are held together by a three-dimensional network of hydrogen bonds. In contrast with compound **1** no  $\text{N}\cdots\text{H}\cdots\text{Cl}$  hydrogen bonds are present connecting

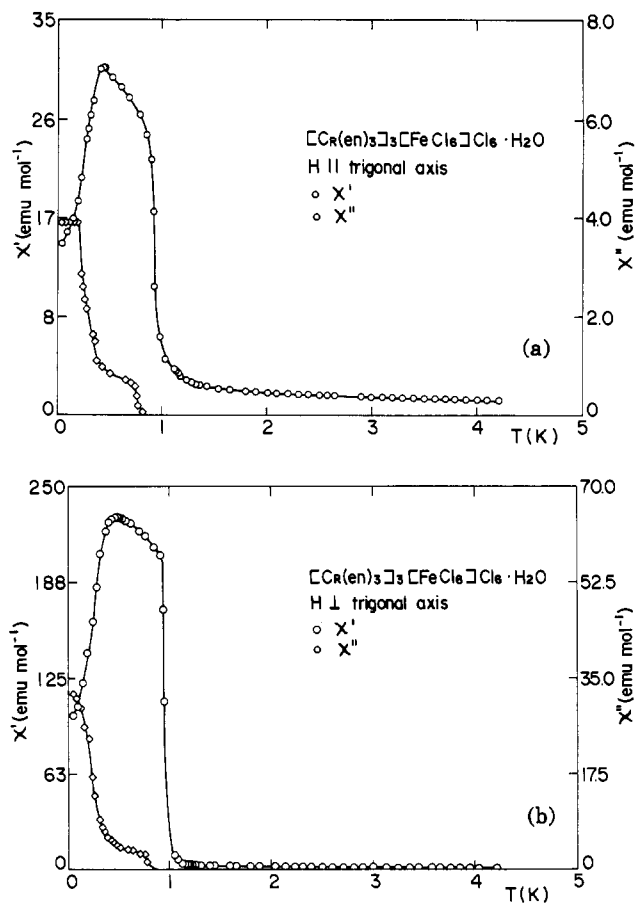


**Figure 4.** AC magnetic susceptibility of a single crystal of  $[\text{Cr}(\text{en})_3]_3[\text{FeCl}_6]\text{Cl}_6 \cdot \text{H}_2\text{O}$  oriented with the alternating field (a) parallel and (b) perpendicular to the trigonal crystallographic axis. Both, the in-phase,  $\chi'$ , and the out-of-phase,  $\chi''$ , components are shown. The solid curve is a guide to the eye.

the  $[\text{Cr}(\text{en})_3]^{3+}$  and  $[\text{FeCl}_4]^-$  complex ions.  $\text{O}\cdots\text{Cl}/\text{N}\cdots\text{O}$  hydrogen bonds relates neighboring  $[\text{FeCl}_4]^-/[\text{Cr}(\text{en})_3]^{3+}$  groups. They are not detected in compound **1**.  $\text{O}\cdots\text{O}$  contacts have also been found.

**Magnetic Properties.**  $[\text{Cr}(\text{en})_3]_3[\text{FeCl}_6]\text{Cl}_6 \cdot \text{H}_2\text{O}$  and  $[\text{Co}(\text{en})_3]_3[\text{FeCl}_6]\text{Cl}_6 \cdot \text{H}_2\text{O}$ . AC magnetic susceptibility data have been carried out on single crystals of **1** and on polycrystalline samples of **2** between 50 mK and 4.2 K while powdered samples of  $[\text{Cr}(\text{en})_3][\text{FeCl}_6]$ ,  $[\text{Co}(\text{en})_3][\text{FeCl}_6]$ , and  $[\text{Cr}(\text{en})_3][\text{InCl}_6]$  have been measured between 1.1 and 4.2 K. Single crystals of  $[\text{Cr}(\text{en})_3]_3[\text{InCl}_6]\text{Cl}_6 \cdot \text{H}_2\text{O}$  were not available, and those of **3** were not large enough for the magnetic study.

The temperature dependence of the in-phase,  $\chi'$ , and out-of-phase,  $\chi''$ , components of the magnetic susceptibility of **1** as measured with the alternating magnetic field parallel,  $\chi_{\parallel}$ , and perpendicular,  $\chi_{\perp}$ , to the trigonal axis are illustrated in Figure 4. At high temperatures the experimental points present a typical paramagnetic behavior. When the temperature decreases, the in-phase component of the susceptibility perpendicular to the trigonal axis,  $\chi'_{\perp}$ , starts increasing very sharply, showing a shoulder at  $0.906 \pm 0.005$  K and a maximum at  $0.475 \pm 0.005$  K, and then declines. The behavior of the parallel component,  $\chi'_{\parallel}$ , is rather similar with a shoulder at about the same temperature as in  $\chi'_{\perp}$  and a maximum at  $0.443 \pm 0.005$  K. Below the temperature at which the shoulder appears, the in-phase component of the susceptibility is accompanied by an out-of-phase signal indicative of the presence of net magnetic moments in the material.<sup>32</sup> Therefore,  $0.906 \pm 0.005$  K can be considered as the temperature at which the compound orders magnetically.

(27) Raymond, K. N.; Meek, D. W.; Ibers, J. A. *Inorg. Chem.* **1968**, *7*, 1111.

(28) Bernal, I.; Korp, J. D.; Schlemper, E. O.; Hussain, M. S. *Polyhedron* **1982**, *1*, 365.

(29) Iwata, M. *Acta Crystallogr. B* **1977**, *33*, 59.

(30) Iwata, M.; Saito, Y. *Acta Crystallogr. B* **1973**, *29*, 822.

(31) Epstein, E. F.; Bernal, I. *J. Chem. Soc. A* **1971**, *22*, 3628.

(32) Palacio, F.; Lazaro, F. J.; van Duyneveldt, A. J. *Mol. Cryst. Liq. Cryst.* **1989**, *176*, 289.

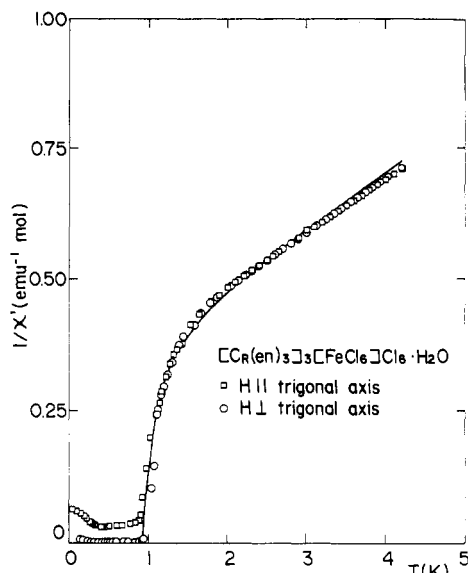


**Figure 5.** Temperature dependence of  $1/\chi'$  as measured in a single crystal of  $[\text{Cr}(\text{en})_3][\text{FeCl}_6]\text{Cl}_6 \cdot \text{H}_2\text{O}$  oriented parallel and perpendicular to the trigonal axis. The continuous line is the theoretical curve (see text).

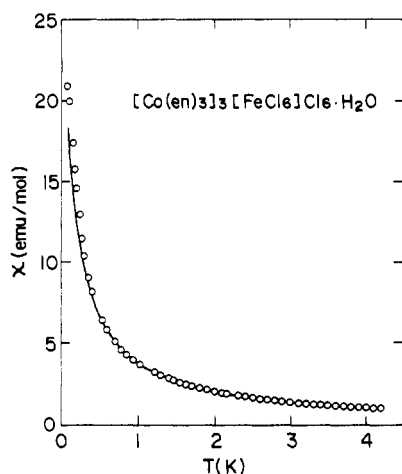


**Figure 6.** Experimental ac magnetic susceptibility of a polycrystalline sample of  $[\text{Co}(\text{en})_3][\text{FeCl}_6]\text{Cl}_6 \cdot \text{H}_2\text{O}$ . The continuous line represents the Curie-Weiss law.

The temperature dependence of  $\chi'^{-1}$  is illustrated in Figure 5. The experimental points at temperatures above 2 K if extrapolated give a negative intercept with the temperature axis, while below 2 K the slope of the  $\chi'^{-1}$  vs  $T$  curve changes abruptly and the extrapolation gives a positive temperature intercept. This is characteristic of ferrimagnetic type behavior arising from the lack of compensation of the two different spin moments present in this compound:  $S = 5/2$  in the octahedral high-spin Fe(III) ion and  $S = 3/2$  in the octahedral Cr(III) ion.

The susceptibility measurements made on a polycrystalline sample of **2** are shown in Figure 6. This compound is paramagnetic down to 0.050 K. No  $\chi''$  signal is observed in this case. The data can be fit to the Curie-Weiss law with  $C_{\text{Fe}} = 4.29 \text{ emu}\cdot\text{K}/\text{mol}$  and  $\theta = -0.1 \text{ K}$ . The only magnetic ion present in **2** is Fe(III) ( $S = 5/2$ ), the Co(III) ions being in low spin ( $S = 0$ ) state. This gives  $\langle g \rangle = 1.98 \pm 0.02$  as calculated from  $C_{\text{Fe}}$ . The small negative value of the parameter  $\theta$  in **2** suggests the presence of weak antiferromagnetic interactions between the Fe ions.

**$[\text{Cr}(\text{en})_3][\text{FeCl}_6]$ ,  $[\text{Co}(\text{en})_3][\text{FeCl}_6]$ , and  $[\text{Cr}(\text{en})_3][\text{InCl}_6]$ .** The susceptibility at zero external magnetic field of a polycrystalline sample of  $[\text{Cr}(\text{en})_3][\text{FeCl}_6]$  measured between 1.1 and 50 K is presented in Figure 7. It is worth remarking the very different magnetic behavior observed in this substance as compared with **1**. At temperatures above approximately 10 K the data can be

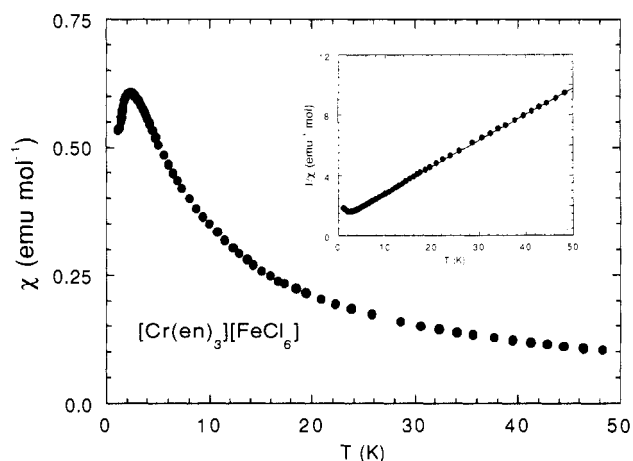


**Figure 7.** Experimental ac magnetic susceptibility of a polycrystalline sample of  $[\text{Cr}(\text{en})_3][\text{FeCl}_6]$ . The insert represents the temperature dependence of  $1/\chi$  and the fit to the Curie-Weiss law.

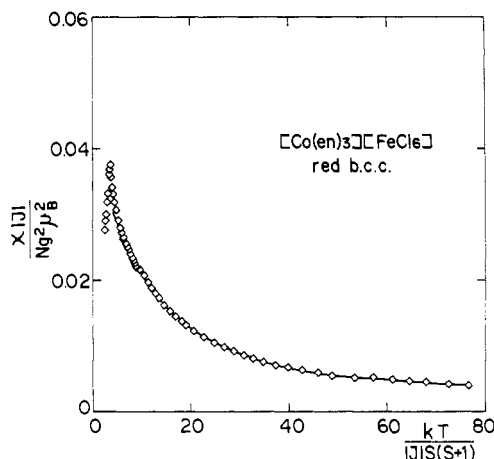


**Figure 8.** Ac magnetic susceptibility of a polycrystalline sample of  $[\text{Co}(\text{en})_3][\text{FeCl}_6]$  in reduced units. The continuous line represents the theoretical fit to a bcc  $S = 5/2$  Heisenberg antiferromagnetic model (see text).

fit to the Curie-Weiss law with  $\theta = -6.9 \text{ K}$  and  $C = 5.88 \text{ emu}\cdot\text{K}/\text{mol}$ . As the temperature decreases, the susceptibility data show a smooth increase, present a maximum at  $2.35 \pm 0.02 \text{ K}$ , and then decrease more rapidly. No out-of-phase component ( $\chi''$ ) is observed over the whole range of temperature. The maximum value of  $d\chi/dT$  is located at  $2.26 \pm 0.02 \text{ K}$ . The magnetic behavior of this compound is really unusual since it is characteristic of an antiferromagnet with ordering temperature  $T_c = 2.26 \text{ K}$  and yet it possesses two different spin values in the magnetic system.

The temperature dependence of the ac magnetic susceptibility of  $[\text{Co}(\text{en})_3][\text{FeCl}_6]$  measured on a polycrystalline sample between 1.1 and 40 K is depicted in reduced units in Figure 8. The only magnetic ion present in this compound is the high-spin Fe(III). At high temperatures the substance follows the Curie-Weiss law with  $C_{\text{Fe}} = 4.38 \text{ emu}\cdot\text{K}/\text{mol}$  ( $\langle g \rangle = 2.00 \pm 0.02$ ) and  $\theta = -2.3 \text{ K}$ . As the temperature decreases, the susceptibility data tends to a maximum at  $1.58 \pm 0.01 \text{ K}$ . No out-of-phase signal is detected over the entire temperature interval. Antiferromagnetic ordering is therefore suggested, the transition temperature  $T_c$  being estimated as  $1.43 \pm 0.01 \text{ K}$  from the maximum value of the positive slope in the susceptibility versus temperature curve.

Magnetic measurements have also been made on a powdered sample of  $[\text{Cr}(\text{en})_3][\text{InCl}_6]$  in the temperature interval between 1.1 and 4.2 K. In this compound the only magnetic ion is  $S = 3/2$  Cr(III) since the In(III) ion is diamagnetic. The compound is paramagnetic and can be fit to a Curie-Weiss law with  $C_{\text{Cr}} = 1.82 \text{ emu}\cdot\text{K}/\text{mol}$ , giving  $\langle g \rangle = 1.97 \pm 0.02$  for  $S = 3/2$  and  $\theta = -0.1 \text{ K}$ .

## Discussion

$[\text{Cr}(\text{en})_3]_3[\text{FeCl}_6]\text{Cl}_6 \cdot \text{H}_2\text{O}$  and  $[\text{Co}(\text{en})_3]_3[\text{FeCl}_6]\text{Cl}_6 \cdot \text{H}_2\text{O}$ . As stated in the previous section, the magnetic behavior of **1** suggests that this compound exhibits ferrimagnetic ordering below  $T_c$ . Because of symmetry, all the chromium ions are equivalent as are all the ferric ions. It is then natural to start considering two magnetic sublattices each formed by respectively the chromium and the iron ions. By the assumption that nearest neighbor interactions, that is between ions of different sublattices, are antiferromagnetic, the resulting magnetic behavior is ferrimagnetic since the magnetic moments of each sublattice do not cancel when they interact with the moments of the other. Using standard molecular field theory for ferrimagnetism,<sup>33</sup> one readily obtains the equation

$$\frac{1}{\chi} = \frac{T^2 - \omega T(\alpha C_A + \beta C_B) - C_A C_B \omega^2 (1 - \alpha\beta)}{(C_A + C_B)T - \omega C_A C_B (2 + \alpha + \beta)} \quad (1)$$

where  $C_A$  and  $C_B$  are the Curie constants of sublattice A and B, respectively,  $\omega = |\gamma_{AB}| = |\gamma_{BA}|$ ,  $\alpha\omega = \gamma_{AA}$ ,  $\beta\omega = \gamma_{BB}$ , and

$$\gamma_{\eta\xi} = \frac{2z_{\eta\xi} J_{\eta\xi}}{N_{\xi} \mu_B^2 g_{\eta} g_{\xi}} \quad \eta = \text{A, B}; \xi = \text{A, B}$$

where  $z_{\eta\xi}$  is the number of nearest neighbors of type  $\xi$  around ion  $\eta$ . This expression for the temperature dependence of  $\chi^{-1}$  can be easily transformed into the well-known Neel hyperbola characteristic of ferrimagnets in the temperature region above  $T_c$ .<sup>34</sup>

It is also useful to derive an equation for the ordering temperature, since  $T_c$  can be established as the point where  $\chi^{-1}$  intercepts the temperature axis. Thus, one obtains

$$T_c = (\omega/2)[\alpha C_A + \beta C_B + (4C_A C_B + (\alpha C_A + \beta C_B)^2)^{1/2}] \quad (2)$$

that gives the theoretical value of  $T_c$  within the molecular field approximation.

In the case of the complex bimetallic salts the versatility in the construction of the magnetic materials, due to the large number of counterions that can be used as building blocks, permits one to obtain the value of the Curie constant for each sublattice independently of the fitting process. Thus, the value of  $C_{\text{Fe}} = 4.288 \text{ emu}\cdot\text{K}/\text{mol}$  for the iron sublattice has been determined from **2** and a typical value of  $C_{\text{Cr}} = 1.848 \text{ emu}\cdot\text{K}/\text{mol}$ <sup>35</sup> has been used for the chromium sublattice, since samples of  $[\text{Cr}(\text{en})_3]_3\text{[InCl}_6]\text{Cl}_6 \cdot \text{H}_2\text{O}$  were not available. A value of  $z_{\text{FeCr}} = z_{\text{FeFe}} = z_{\text{CrCr}} = 6$  has been derived from the analysis of the superexchange pathways as we explain below, and the values of  $N_{\text{Fe}} = N_0$  and  $N_{\text{Cr}} = 3N_0$  are readily obtained from the chemical formula.  $N_0$  represents Avogadro's number.

The high-temperature data for **1** (see Figure 5) show no anisotropy between the measurements parallel and perpendicular to the 3-fold axis direction. This is the behavior expected for such isotropic ions as Cr(III) and Fe(III). Then, fitting the experimental points to eq 1 gives  $J_{\text{Fe-Cr}}/k_B = -0.153 \pm 0.007 \text{ K}$ ,  $J_{\text{Fe-Fe}}/k_B = -0.044 \pm 0.005 \text{ K}$ , and  $J_{\text{Cr-Cr}}/k_B = -0.045 \pm 0.004 \text{ K}$ . Demagnetization correction was found to affect these results within experimental error, since only data from the paramagnetic region have been considered in the fit. At this point, it is advisable to take into account that molecular field theory tends to overestimate intrasublattice magnetic interactions.<sup>36-38</sup> Then, a

collinear ferrimagnetic structure cannot be disregarded from the negative values of the  $J_{\text{Fe-Fe}}/k_B$  and  $J_{\text{Cr-Cr}}/k_B$  superexchange constants.<sup>34</sup> From eq 2 an ordering temperature of 0.96 K is obtained in good agreement with 0.91 K, the temperature at which the first maximum appears in the susceptibility data. On the other hand, spin reorientations cannot be disregarded and this might be the origin of the maximum that both  $\chi_{\parallel}$  and  $\chi_{\perp}$  exhibit below  $T_c$ . More information coming from complementary techniques, such as neutron diffraction, would be necessary to understand the exact nature of such a maximum.

In order to understand better the magnetic behavior of this compound we have analyzed the superexchange interaction pathways. A reference Fe(III) ion is connected to six Cr(III) nearest neighbors (at an average distance of 8 Å) by  $\text{Fe}^{2.4\text{Å}}\text{Cl}^{3.3-3.5\text{Å}}\text{N}^{2.1\text{Å}}\text{Cr}$  bridges, where Cl...N are hydrogen bonded. Next-nearest Cr(III) ions are at a much larger distance (about 12 Å) from the reference Fe(III). Consequently, next-nearest neighbor (nnn) interactions are expected to be much smaller than nearest-neighbor (nn) ones. In addition, a reference Cr(III) ion interacts with six Cr(III) nearest magnetic neighbors, which are located at about 9 Å from the reference Cr(III), through superexchange paths  $\text{Cr}^{2.1\text{Å}}\text{N}^{4.0-4.6\text{Å}}\text{N}^{2.1\text{Å}}\text{Cr}$ . This non-bonding interaction between the nitrogen atoms could be enhanced by the presence of N...Cl hydrogen bonds (the chlorine atom not being bonded to a ferric ion) giving rise to an additional magnetic superexchange path  $\text{Cr}^{2.1\text{Å}}\text{N}^{3.2-3.4\text{Å}}\text{Cl}^{3.2-3.4\text{Å}}\text{N}^{2.1\text{Å}}\text{Cr}$ , where the chromium ions are now at an average distance of 11 Å. Finally, each Fe(III) ion is connected to its six Fe(III) nn, by superexchange paths  $\text{Fe}^{2.4\text{Å}}\text{Cl}^{3.1-3.2\text{Å}}\text{Cl}^{2.4\text{Å}}\text{Fe}$ . The iron-iron average distance is about 13 Å.

The distance between two Fe(III) nearest neighbors is too large to expect a nonnegligible magnetic interaction between the ferric ions. The superexchange pathway is much more favorable in the case of intersublattice contacts, the interaction between the Fe(III) and Cr(III) ions being highly enhanced by the presence of N-H...Cl hydrogen bonds. This is not the case for the Cr(III) sublattice since there is not a bonding interaction between the N atoms involved in the corresponding superexchange pathway. These conclusions are in good agreement with the experimental values obtained for the magnetic superexchange constants.

Similar superexchange pathways can be found in the bimetallic compound  $[\text{Cr}(\text{H}_2\text{O})(\text{NH}_3)_5][\text{FeCl}_6]$ .<sup>39</sup> Therefore, the values found for  $J_{\text{Fe-Cr}}$  and  $J_{\text{Cr-Cr}}$  are similar for both compounds.<sup>19</sup> However,  $J_{\text{Fe-Fe}}/k_B$  is significantly higher for  $[\text{Cr}(\text{H}_2\text{O})(\text{NH}_3)_5][\text{FeCl}_6]$  than for **1** (0.12 K vs 0.04 K). The fact that two Fe<sup>3+</sup> nearest-neighbor ions are notably more separated in **1** than in  $[\text{Cr}(\text{H}_2\text{O})(\text{NH}_3)_5][\text{FeCl}_6]$  (13 Å vs 9 Å) certainly contributes to this difference.

Hydrogen bonds have been observed before to participate in the superexchange pathways of simple systems by connecting isolated coordination octahedra.<sup>40-42</sup> More subtle is the role hydrogen bonds play in other more complex molecular ferromagnets, where they contribute to transmit interchain magnetic interactions.<sup>43-45</sup> However, to the best of our knowledge, the active role played by hydrogen bonds in the magnetic ordering of complex bimetallic salts has not been considered previously.

With respect to compound **2**, it remains paramagnetic in the whole range of temperature measured (50 mK–4.2 K) as expected

(33) Herpin, A. *Theory of Magnetism*; Presses Universitaires de France: Paris, 1968.

(34) Neel, L. *Ann. Phys., Paris* **1948**, *3*, 137.

(35) Carlin, R. L. *Magnetochemistry*; Springer-Verlag: New York, 1986.

(36) Smit, J.; Wijn, P. J. *Ferrites*; John Wiley & Sons: New York, 1956; pp 24–27.

(37) Smart, J. S. *Magnetism*; Academic Press: New York, 1963; Vol. III, p 103.

(38) Lüthi, B. *Phys. Rev.* **1966**, *148*, 519.

(39) Morón, M. C.; Palacio, M. C.; Pons, J.; Casabó, J. To be published.

(40) Puertolas, J. A.; Navarro, R.; Palacio, F.; Bartolome, J.; Gonzalez, D. *Phys. Rev. B* **1985**, *31*, 516.

(41) Carlin, R. L.; Burriel, R. *Phys. Rev. B* **1983**, *27*, 3012.

(42) Carlin, R. L.; Palacio, F. *Coord. Chem. Rev.* **1985**, *165*, 141.

(43) Kahn, O.; Pei, Y.; Verdager, M.; Renard, J. P.; Sletten, J. J. *Am. Chem. Soc.* **1988**, *110*, 782.

(44) Nakatani, K.; Carriat, J. Y.; Journaux, Y.; Kahn, O.; Lloret, F.; Renard, J. P.; Pei, Y.; Sletten, J.; Verdager, M. *J. Am. Chem. Soc.* **1989**, *111*, 5739.

(45) Pei, Y.; Kahn, O.; Nakatani, K.; Codjovi, E.; Mathoniere, C.; Sletten, J. J. *Am. Chem. Soc.* **1991**, *113*, 6558.

from the very unfavorable superexchange path  $\text{Fe} \xrightarrow{2.4 \text{ \AA}} \text{Cl} \xrightarrow{8.0-8.2 \text{ \AA}} \text{Cl} \xrightarrow{2.4 \text{ \AA}} \text{Fe}$ . The parameter  $\theta = -0.1 \text{ K}$  for **2** allows us to calculate the exchange constant in this material. Within the experimental error, we find  $J_{\text{Fe-Fe}}/k_B = 0$ , which explains why the compound remains paramagnetic down to 50 mK.

**[Cr(en)<sub>3</sub>][FeCl<sub>6</sub>]** and **[Cr(en)<sub>3</sub>][FeCl<sub>4</sub>]Cl<sub>2</sub>·9H<sub>2</sub>O**. In contrast with the previous Cr/Fe compound, **[Cr(en)<sub>3</sub>][FeCl<sub>6</sub>]** seems to behave as an antiferromagnet. Such striking magnetic behavior has been predicted to arise as a consequence of strong intrasublattice antiferromagnetic interactions.<sup>33,46</sup> The behavior has been experimentally observed in  $\text{Mn}_2\text{Mo}_3\text{O}_8$ , a system with one type of magnetic ion in two nonequivalent crystallographic sites.<sup>47</sup> To the authors' knowledge **[Cr(en)<sub>3</sub>][FeCl<sub>6</sub>]** could be the first material possessing two different spins in which such magnetic properties are observed. Another Cr/Fe compound, **[Cr(NH<sub>3</sub>)<sub>6</sub>][FeCl<sub>6</sub>]**, initially reported as ferrimagnetic<sup>12</sup> might in fact also behave as an antiferromagnet when none of the ammonia present in the sample is substituted by water molecules.<sup>48-50</sup>

The knowledge of the crystal structure of **[Cr(en)<sub>3</sub>][FeCl<sub>6</sub>]** would be desirable to corroborate if the superexchange pathways support such strong intrasublattice ( $J_{\text{intra}}$ ) versus intersublattice ( $J_{\text{inter}}$ ) interactions. Interestingly enough, no N...Cl hydrogen bonds can be found in the magnetic pathway Fe-Cl-N-Cr in **[Cr(en)<sub>3</sub>][FeCl<sub>4</sub>]Cl<sub>2</sub>·9H<sub>2</sub>O** (see Crystal Structures section), which would not certainly contribute to increase  $J_{\text{inter}}$  in this compound. By the contrary, the presence of N...Cl hydrogen bonds in the intersublattice superexchange pathway of **1** surely helps to increase the intensity of  $J_{\text{inter}}$  and therefore that of  $J_{\text{inter}}/J_{\text{intra}}$ . As a result, although  $J_{\text{Fe-Fe}}$  and  $J_{\text{Cr-Cr}}$  are antiferromagnetic in character, no compensate ferrimagnetic ordering is observed in **1**.

**[Co(en)<sub>3</sub>][FeCl<sub>6</sub>]** and **[Cr(en)<sub>3</sub>][InCl<sub>6</sub>]**. **[Co(en)<sub>3</sub>][FeCl<sub>6</sub>]** orders as an antiferromagnet at  $T_c = 1.43 \pm 0.01 \text{ K}$ . A similar behavior has been observed in **[Co(pn)<sub>3</sub>][FeCl<sub>6</sub>]** (pn = 1,2-propanediamine). Although pn is bulkier than en, the latter compound orders at a much higher temperature,  $T_c = 8.15 \pm 0.05 \text{ K}$ .<sup>11</sup> Unfortunately, no single crystals of these compounds are available to solve the crystal structure and to study the possible magnetic superexchange paths in order to understand the origin of this striking difference. The knowledge of the crystal structure of **[Co(en)<sub>3</sub>][FeCl<sub>6</sub>]** would also permit one to establish a simple magnetic model to fit the magnetic properties of the compound. In the absence of such a model we have fit the magnetic susceptibility data to both a sc and a bcc  $S = 5/2$  Heisenberg antiferromagnet using high-temperature series expansions<sup>51</sup> extrapolated with Padé approximants.<sup>52</sup> The fit gives similar, for  $g = 2.00 \pm 0.02$ , exchange constant values of  $J/k_B = 0.067 \pm 0.005 \text{ K}$  for the sc lattice and  $J/k_B = 0.050 \pm 0.005 \text{ K}$  for the bcc one. The fitting of the susceptibility to the bcc lattice model is shown as a representative example in Figure 8.

**[Cr(en)<sub>3</sub>][InCl<sub>6</sub>]** remains paramagnetic down to 1.1 K. This is not surprising since coordination compounds of octahedral  $\text{Cr}^{3+}$  ion are known to order at very low temperatures.<sup>53</sup>

## Conclusions

Unusual and rich magnetic behavior can be observed in the series of compounds formed by  $[\text{M}(\text{en})_3]^{3+}$  ( $\text{M} = \text{Cr}, \text{Co}$ ) and  $[\text{M}'\text{Cl}_6]^{3-}$  ( $\text{M}' = \text{Fe}, \text{In}$ ) counterions. In this line, we have stated the interest of dealing with different counterions to be used as building blocks in the construction of the magnetic materials.

In the determination of the type of magnetic ordering that these complex bimetallic compounds could exhibit, it is important to consider not only the pair of transition metal ions involved but also the particular superexchange pathway connecting them. Thus, **[Cr(en)<sub>3</sub>][FeCl<sub>6</sub>]Cl<sub>6</sub>·H<sub>2</sub>O** orders as a ferrimagnet but **[Cr(en)<sub>3</sub>][FeCl<sub>6</sub>]** exhibits an antiferromagnetic-like (compensated ferrimagnetic) ordering. In particular, the type of superexchange pathways shown by these bimetallic compounds favors the ferrimagnet **[Cr(en)<sub>3</sub>][FeCl<sub>6</sub>]Cl<sub>6</sub>·H<sub>2</sub>O** to exhibit a low critical temperature  $T_c$ . Low-temperature ferrimagnets are rather unusual and interesting since they permit accurate thermodynamic studies.

The relevance of the intermolecular magnetic interactions in determining the magnetic behavior of these complex bimetallic compounds has been shown. In this paper, hydrogen bonds are shown to participate effectively in the propagation of the superexchange interaction between magnetic sublattices constituting an effective mechanism to propagate magnetic interaction in molecular magnets.

More information coming from other techniques is necessary to understand these complicated magnetic materials. Neutron diffraction is certainly the most definitive technique in this case, although techniques such as magnetization, specific heat, and Mössbauer spectroscopy can also be of considerable help to better understand these phenomena.

## Experimental Section

**Chemical Synthesis.** Single crystals of **[Cr(en)<sub>3</sub>][FeCl<sub>6</sub>]Cl<sub>6</sub>·H<sub>2</sub>O** were prepared by addition of an aqueous solution of ferric chloride to **[Cr(en)<sub>3</sub>]Cl<sub>3</sub>** (1:1 molar ratio) yielding an aqueous solution which was partially evaporated. Concentrated hydrochloric acid was added, and slow evaporation led to nice deep-red crystals in a few days. In a similar way the analogous Co derivative was prepared.

To prepare the compound **[Cr(en)<sub>3</sub>][FeCl<sub>6</sub>]**, a solution of 3.9 g of  $\text{FeCl}_6 \cdot 6\text{H}_2\text{O}$  in 5 mL of hot, concentrated HCl was added to a solution of 0.5 g of **[Cr(en)<sub>3</sub>]Cl<sub>3</sub>** in 5 mL of water. After several minutes a yellow-orange precipitate appeared, which was filtered out, washed with isopropyl alcohol, and vacuum dried. In a similar way the **[Co(en)<sub>3</sub>][FeCl<sub>6</sub>]** and the **[Cr(en)<sub>3</sub>][InCl<sub>6</sub>]** analogs were prepared. The elemental analyses, available as supplementary material (Table S11), were satisfactory.

Several attempts were made to grow single crystals of **[Cr(en)<sub>3</sub>][FeCl<sub>6</sub>]** and **[Co(en)<sub>3</sub>][FeCl<sub>6</sub>]** by increasing the Fe/M ( $\text{M} = \text{Cr}, \text{Co}$ ) molar ratio in the hydrochloric solution. Only in the case of the first compound could we successfully obtain some crystals of a substance with the 1:1 stoichiometry suitable for X-ray structural determination. The correct formula corresponding to the compound in the crystal was found to be **[Cr(en)<sub>3</sub>][FeCl<sub>4</sub>]Cl<sub>2</sub>·9H<sub>2</sub>O**.

**X-ray Data.** **[Cr(en)<sub>3</sub>][FeCl<sub>6</sub>]Cl<sub>6</sub>·H<sub>2</sub>O**. A dark red tabular crystal ( $0.15 \times 0.15 \times 0.20 \text{ mm}^3$ ) was selected and mounted on an Enraf-Nonius CAD4 diffractometer. Accurate cell parameters were determined from the centering of 25 reflections. The data were collected with graphite-monochromatized  $\text{Mo K}\alpha$  radiation, using the  $\omega$  scan technique. A total of 1723 reflections were collected in the range  $1^\circ \leq \theta \leq 25^\circ$ , 1020 of which with intensity greater than  $3\sigma(I_0)$  were used for the least-squares refinement of 171 parameters.

**[Co(en)<sub>3</sub>][FeCl<sub>6</sub>]Cl<sub>6</sub>·H<sub>2</sub>O**. A dark red tabular crystal ( $0.2 \times 0.2 \times 0.1 \text{ mm}^3$ ) was selected and mounted on a Philips PW-1100 four-circle diffractometer. Unit cell parameters were determined from automatic centering of 25 reflections ( $4^\circ \leq \theta \leq 12^\circ$ ) and refined by the least-squares method. Intensities were collected with graphite-monochromatized  $\text{Mo K}\alpha$  radiation, using the  $\omega$  scan technique. A total of 2932 reflections were measured in the range  $2^\circ \leq \theta \leq 25^\circ$ , 2584 of which with intensity greater than  $2.5\sigma(I_0)$  were used for least-squares refinement of 171 parameters.

**[Cr(en)<sub>3</sub>][FeCl<sub>4</sub>]Cl<sub>2</sub>·9H<sub>2</sub>O**. An equidimensional yellow crystal ( $0.7 \times 0.7 \times 0.7 \text{ mm}^3$ ) was selected and mounted on the above mentioned Philips diffractometer with the same experimental conditions described for **2**, except that a total of 1343 reflections were measured, 864 of which were used for least-squares refinement of 95 parameters.

In the three cases, the Fe and Cr (or Co) atoms were located from Patterson syntheses while a Fourier synthesis were used to locate the remaining non-hydrogen atoms. Refinement was made by the full-matrix least-squares method, using the SHELX76 computer program.<sup>54</sup>  $f, f',$

(46) Yafet, Y.; Kittel, C. *Phys. Rev.* **1952**, *87*, 290.

(47) McAlister, S. P. *J. Appl. Phys.* **1984**, *55*, 2343.

(48) Morón, M. C. Thesis, University of Zaragoza, 1988.

(49) Reiff, W. M. *Hyper. Inter.* **1988**, *40*, 195.

(50) Palacio, F.; Morón, M. C.; Pons, J.; Casabó, J.; Carlin, R. L. To be published.

(51) Rushbrooke, G. S.; Baker, Jr., G. A.; Wood, J. In *Phase Transitions and Critical Phenomena*; Domb, C., Green, M. S., Eds.; Academic Press: London, 1974; Vol. III, p 246.

(52) Navarro, R. Thesis, University of Zaragoza, 1976.

(53) Merabet, K. E.; Burriel, R.; Carlin, R. L. *Phys. Rev. B* **1988**, *38*, 11589.

and  $f''$  were taken from the *International Tables of X-ray Crystallography*. The final  $R$  factors, unit cells, and space groups are shown in Table 1.

**Magnetic Susceptibility Data.** Ac magnetic susceptibility measurements at zero external magnetic field and 120 Hz were made between 1.1 K and 40 K using conventional techniques.<sup>55-57</sup> The ac susceptibility measurements between 50 mK and 4.2 K were performed at 16 Hz using a  $^3\text{He}/^4\text{He}$  dilution refrigerator.<sup>58</sup>

**Acknowledgment.** The research in Zaragoza and Barcelona has been supported respectively by Grants 3380/83, 409/84, MAT88/0174, and MAT91/681 from the Comisión Asesora de

Investigación Científica y Técnica of the Ministerio de Educación y Ciencia. The research in Chicago has been supported by Grant DMR-8515224 and DMR-8815798 from the Solid State Chemistry Program, Division of Materials Research of the National Science Foundation. The cooperative work has been supported by Grant CCB-8504/001 from the American-Spain Joint Committee for Technical and Scientific Cooperation.

**Supplementary Material Available:** Additional crystallographic information about compounds 1-3 including tables containing complete crystal data collection and structure refinement parameters (Table S1), atomic coordinates (Tables S2-S4), main interatomic distances and angles (Tables S5-S7), and anisotropic temperature factors (Tables S8-S10) and a table of elemental analysis results for  $[M(en)_3][M'Cl_6]$  ( $M = \text{Cr}, \text{Co}; M' = \text{Fe}, \text{In}$ ) (Table S11) (10 pages). Ordering information is given on any current masthead page.

- 
- (54) Sheldrick, G. M. *SHELX: A Computer Program for Crystal Structure Determination*; Univ. of Cambridge: Cambridge, U.K., 1976.  
(55) Bhatia, S. N.; Carlin, R. L.; Paduan Filho, A. *Physica B* 1977, 92, 330.  
(56) Rillo, C. Thesis, University of Zaragoza, Spain, 1986.  
(57) Rillo, C.; Lera, F.; Badía, A.; Angurel, L. A.; Bartolomé, J.; Palacio, F.; Navarro, R.; van Duyneveldt, A. J. In *Magnetic Susceptibility of Superconductors and other Spin Systems*; Hein, R. A., Francavilla, T. L., Liedenberg, D. H., Eds.; Plenum Press: New York, 1991; p 1.

- 
- (58) van der Bilt, A.; Joung, K. O.; Carlin, R. L.; de Jongh, L. J. *Phys. Rev. B* 1980, 22, 1259.